Plant, Cell and Environment (2006) **29**, 483–496 doi: 10.1111/j.1365-3040.2005.01425.x

Using continuous stable isotope measurements to partition net ecosystem CO_2 exchange

JIANMIN ZHANG[1], TIMOTHY J. GRIFFIS[1] & JOHN M. BAKER[1,2]

[1]*Department of Soil, Water, and Climate, University of Minnesota-Twin Cities, 439 Borlaug Hall, 1991 Upper Buford Circle, St. Paul, MN 55108, USA and* [2]*USDA-ARS, 439 Borlaug Hall, 1991 Upper Buford Circle St. Paul, MN 55108, USA*

ABSTRACT

Ecosystem-scale estimation of photosynthesis and respiration using micrometeorological techniques remains an important, yet difficult, challenge. In this study, we combined micrometeorological and stable isotope methods to partition net ecosystem CO_2 exchange (F_N) into photosynthesis (F_A) and respiration (F_R) in a corn–soybean rotation ecosystem during the summer 2003 corn phase. Mixing ratios of $^{12}CO_2$ and $^{13}CO_2$ were measured continuously using tunable diode laser (TDL) absorption spectroscopy. The dynamics of the isotope ratio of ecosystem respiration (δ_R), net ecosystem CO_2 exchange (δ_N) and photosynthetic discrimination at the canopy scale (Δ_{canopy}) were examined. During the period of full canopy closure, F_N was partitioned into photosynthesis and respiration using both the isotopic approach and the conventional night-time-derived regression methodology. Results showed that δ_R had significant seasonal variation (–32 to –11‰) corresponding closely with canopy phenology. Daytime δ_N typically varied from –12 to –4‰, while Δ_{canopy} remained relatively constant in the vicinity of 3‰. Compared with the regression approach, the isotopic flux partitioning showed more short-term variations and was considerably more symmetric about F_N. In this experiment, the isotopic partitioning resulted in larger uncertainties, most of which were caused by the uncertainties in δ_N and the daytime estimate of δ_R. By sufficiently reducing these uncertainties, the tunable diode laser (TDL)–micrometeorological technique should yield a better understanding of the processes controlling photosynthesis, respiration and ecosystem-scale discrimination.

Key-words: discrimination; isotopic disequilibrium; Keeling plot; partition; photosynthesis.

INTRODUCTION

Studies of stable isotope variation and exchange between ecosystems and the atmosphere can provide new insight into biological and physical controls on carbon cycling. Stable isotope analyses have been used to identify global carbon sources and sinks (Ciais *et al*. 1995; Lloyd, Krujit & Hollinger 1996; Fung *et al*. 1997; Battle *et al*. 2000), to partition ecosystem CO_2 respiration (Flanagan & Ehleringer 1997; Rochette, Flanagan & Gregorich 1999), and particularly to partition the net ecosystem exchange of CO_2 (F_N) into photosynthesis (F_A) and respiration (F_R) (Yakir & Wang 1996; Hanson *et al.* 2000; Bowling, Tans & Monson 2001; Lai *et al*. 2003; Ogée *et al*. 2003). At present, F_N is measured globally as part of the global FLUXNET network with the eddy covariance (EC) technique. However, measuring F_A and F_R directly remains an important and difficult challenge. Traditionally, F_R is estimated using night-time-derived temperature regression models (Ruimy, Jarvis & Baldocchi 1995; Goulden *et al*. 1997), and F_A is estimated using daytime light-response analyses (Falge *et al*. 2002; Griffis *et al*. 2003). However, these approaches may not adequately account for the physiological controls on respiration that are likely to differ between day and night (Brooks & Farquhar 1985; Janssens *et al*. 2001). Automated chambers have been used to quantify half-hourly values of component respiration and have been scaled up to the ecosystem (Drewitt *et al*. 2002; Griffis *et al*. 2004a), but the results have substantial uncertainty because of the relatively large spatial variation and limited number of chambers deployed. The chamber scaling also requires temperature-dependent algorithms. Single-layer and multilayer canopy models (Baldocchi & Harley 1995; Wang & Leuning 1998) have also been used in estimating F_A. These physiological models usually require detailed canopy structure information and assumptions regarding scales that we ultimately want to test with the best available ecosystem-scale data. The parameterization of these models might be very specific to certain types of ecosystems, which further limits their universal application.

The stable isotope technique provides an independent methodology for short-term F_N partitioning. Applying the mass balance principle, Yakir & Wang (1996) have partitioned F_N using measurements of CO_2 concentration and the isotope ratios of plant, soil and atmosphere over an agricultural ecosystem. However, their method is only applicable over relatively long timescales because the isotope ratios of plants and bulk soil organic matter represent integrative values and therefore do not explicitly account for the short-term dynamics of F_A or F_R. Through the combination of isotopic and micrometeorological techniques, Bowling *et al*. (2001) improved upon the methodology of

Correspondence: Jianmin Zhang. Fax: +1 612 625 2208; e-mail: jzhang@umn.edu

© 2005 Blackwell Publishing Ltd

Yakir & Wang (1996) by introducing short-term (i.e. half-hourly) canopy scale photosynthetic discrimination (Δ_{canopy}) and by quantifying the isoflux [isoflux = $\rho\overline{w'(\delta_a C_a)'}$, where ρ is molar air density, w is vertical wind speed, C_a is CO_2 mixing ratio, δ_a is the isotope ratio of ambient air, primes denote fluctuations from the mean and the overbar denotes time averaging], which is an isotopic approximation of the vertical flux of $^{13}CO_2$. This methodology has also been applied to the partitioning of the F_N of a C_4-dominated grassland (Lai *et al*. 2003) and a temperate coniferous forest (Ogée *et al*. 2003).

In the isotopic flux partitioning, the isotope ratio of ecosystem respiration (δ_R) and the isoflux (or approximately, $\delta_N \cdot F_N$, where δ_N is the isotope ratio of F_N) are the two critical parameters that need to be determined. Traditionally, δ_R has been estimated using the Keeling plot method, which is based on the linear relationship between the isotope ratio and the reciprocal of the CO_2 mixing ratio (Keeling 1958). However, the Keeling plot method is subject to a number of uncertainties. These include advection, variation in the isotopic composition of the background atmosphere and the extrapolation of CO_2 mixing ratio to a value well beyond the usually narrow range of observation (Ogée *et al*. 2003; Pataki *et al*. 2003; Griffis *et al*. 2004b). Bowling *et al*. (2001) have estimated the isoflux using a Keeling-type function that has been tested over various timescales. However, this function might have considerable uncertainty when the CO_2 range is narrow, which typically occurs during the daytime (Ogée *et al*. 2004). δ_N has been estimated as the slope of the regression between ($\delta_a C_a - \delta_{bg} C_{bg}$) and ($C_a - C_{bg}$), where C_{bg} and δ_{bg} are the assumed CO_2 mixing ratio and the isotope ratio of the background atmosphere, respectively (Lai *et al*. 2004; Ogée *et al*. 2004). This approach is sensitive to the values chosen for C_{bg} and δ_{bg} and might not be appropriate for field-scale studies because of boundary layer dynamics.

The above partitioning studies relied on flask sampling and mass spectrometry laboratory analyses, limiting their temporal resolution. With the recent development of tunable diode laser (TDL) spectroscopy, continuous observation of stable isotopomer mixing ratios ($^{12}CO_2$ and $^{13}CO_2$) at high temporal resolution is now possible (Bowling *et al*. 2003). Griffis *et al*. (2004b) have estimated δ_R based on two-level gradient measurements of $^{12}CO_2$ and $^{13}CO_2$ using the TDL technique. This gradient approach (also referred to as the flux ratio method) can be used to obtain short-term, dynamic estimates of δ_R and is less dependent on the variation of the background atmosphere. Their study carried out over a harvested agricultural ecosystem (Griffis *et al*. 2004b) showed that the gradient approach generally agreed well with the Keeling plot method on δ_R estimation but had larger uncertainty because of the relatively small fluxes during the measurement period (November in Minnesota). However, this method requires further testing during growing season conditions when fluxes are greater.

Therefore, the objectives of this paper are: (1) to examine the short-term dynamics of δ_R and δ_N determined with the flux ratio method; (2) to partition F_N of a C_3–C_4 rotation agricultural ecosystem using mass balance principles by combining TDL and micrometeorological measurements; and (3) to explore the uncertainties of the isotopic partitioning approach and present recommendations for future studies.

MATERIALS AND METHODS

Site

The experiment was conducted in a 17 ha corn (*Zea mays* L., C_4 photosynthetic pathway) field from 21 May to 14 October [day of year (DOY) 141–287] 2003 at the Rosemount Research and Outreach Center of the University of Minnesota, 24 km south of St. Paul (44°42′N, 93°05′W, elevation of 259.8 m.a.s.l.). The pre-settlement vegetation of the site was upland dry prairie, with conversion to agriculture occurring approximately 125 years ago (Griffis, Baker & Zhang 2005). The site, which had been in continuous corn production during the previous 4 years, was planted with soybeans (*Glycine max*, C_3 photosynthetic pathway) in 2002. The site is flat and homogenous with a fetch of about 200 m in all directions. The soil is predominantly a Waukegan silt loam with an average bulk density of 1.25 g cm^{-3}. The isotopic composition of the soil organic matter ranges from about −15.1‰ at a depth of 90 cm to −18.0‰ at a depth of 5 cm (Griffis *et al*. 2005).

Micrometeorological measurements

The details of the instrumentation and field set-up have been well documented by Griffis *et al*. (2004b) and Baker & Griffis (2005). The mixing ratios of $^{12}CO_2$ and $^{13}CO_2$ (μmol CO_2 mol^{-1} dry air) were measured with the TDL technique (TGA100, Campbell Scientific Inc., Logan UT, USA). The instrument was maintained in a temperature-controlled research trailer approximately 200 m from the instrument tower. Three air inlets, one inside the canopy and two above the canopy, were mounted on the tower and were connected with Synflex tubing (Synflex Type 1300, Aurora, OH) to the TDL manifold. Each air inlet was composed of a Delrin 25 mm filter with Teflon filter membranes (A-06623-32 and EW-02916-72, Cole-Parmer, Vernon Hills, IL, USA) and a brass critical flow orifice (model D-7-BR, O'Keefe Controls Co., Monroe, CT, USA) that controlled the flow rate at 0.260 L min^{-1}. The heights of the inlets were adjusted according to canopy development, but the separation between the two inlets above the canopy remained at 0.65 m over the experimental period. Air was pulled through a Nafion Dryer (PD-200T-24SS, Perma Pure Inc., Toms River, NJ, USA) into the TDL sample cell by a vacuum pump (Busch Rotary Vane Vacuum Pump, RB0021-L, Busch Inc., Shropshire, UK). A solenoid manifold, controlled by the TDL software, was used to select each intake line. A CO_2 reference gas with approximately 10% $^{12}CO_2$ and 1% $^{13}CO_2$ flowed through the reference cell at a rate of 10 mL min^{-1}. The reference cell signal is used only to provide a spectral template, thus the concentration need

not be known with high precision. Two gases with known total CO_2 mixing ratio (351.84 and 657.11 μmol mol^{-1}) and isotope ratio (–14.43 and –14.36‰) were used to calibrate the TDL every 2 min. These working standards were propagated by using NOAA-CMDL primary standards to calibrate unknown cylinders for mixing ratios of isotopomers with the TDL (Griffis *et al*. 2004b). The sampling algorithm cycled through two calibration gases and then four air inlets (the fourth inlet was positioned for zero gradient testing) in 2 min. Each line was sampled for 20 s at 10 Hz, with the first 7 s of measurement omitted for pressure equilibration and the next 13 s of measurement averaged as the mean of the 2 min period. Small sample cell pressure differences between the calibration tank and the field inlets were observed. The average sample cell pressure of the two inlets measured above the canopy over the entire period was approximately 14.4 and 16.9 Pa, respectively. Pressure testing indicated that the effect of pressure fluctuation on the isotope ratio measurement was random, about 0.0059‰ per Pa. Thus, the observed pressure difference between the calibration tank and the field inlets would cause a ± 0.08‰ and ± 0.10‰ variation on the 2 min δ_a measurement for the two inlets above the canopy, respectively, and a negligible influence on the δ_N and δ_R estimated with the flux ratio method (< 0.001‰).

A 3-D sonic anemometer–thermometer (CSAT3, Campbell Scientific Inc.) and an open-path infrared gas analyser (LI-7500, Li-Cor Inc., Lincoln, NE, USA) were mounted on the same tower as the TDL sample inlets. The EC system was positioned at a height of 2 m above the ground when the canopy was less than 1 m high. The height of the EC system was then adjusted upward as the crop grew. For most of the experimental period, the EC system was at the centre of the two TDL inlets above the canopy. The fluxes of sensible heat (H), latent heat (λE) and CO_2 were derived from the half-hourly mean covariance of the fluctuation of vertical wind speed (w') and the fluctuations of air temperature (T_a'), water vapour density (q') and CO_2 concentration (C'), respectively. The EC system sampled all signals at 10 Hz and stored half-hourly statistics to a datalogger (Campbell CR23X, Campbell Scientific Inc.).

Downwelling and upwelling solar and long-wave radiation were measured with upward- and downward-facing pyranometers and pyrgeometers, respectively (models 8–48 and PIR, Eppley Laboratory Inc., Newport, RI, USA), mounted in close proximity at a height of 3 m from the soil surface. Net radiation (R_n) was computed as the sum of these four component measurements. Soil heat flux was measured with two self-calibrating heat flux plates (HFP01SC, Hukseflux Thermal Sensors, Delft, the Netherlands) at a depth of 10 cm. The mean soil temperature in the 10 cm layer above the heat flux plate was averaged from the measurements of three thermocouples buried at depths of 1.5, 5 and 8.5 cm. The soil heat capacity was measured by a dual needle probe custom made by Thermal Logic Devices (Pullman, WA, USA). The soil heat flux was corrected for heat storage in the top 10 cm layer. The radiation and heat flux data were recorded on a separate datalogger (Campbell 21X, Campbell Scientific Inc.). Weekly leaf area index (LAI) was measured with an AccuPAR handheld sensor (AccuPAR, Model PAR-80, Decagon Devices Inc., Pullman, WA, USA).

Analysis of plant carbon isotope ratio

Green corn leaves were collected every 2 weeks for isotope analysis. Fifteen plants were randomly collected from three plots. The leaves were cleaned and oven dried at 60 °C for at least 48 h until the mass remained constant. Samples were ground to a fine powder with a ball mill (5300 Mixer/Mill, Spex Industries, Edison, NJ, USA). A subsample of approximately 2 mg was weighed into a foil capsule and analysed for the isotope ratio on a continuous flow model mass spectrometer (Optima, Waters Corporation, Milford, MA, USA). The isotope analysis was expressed as an isotopic ratio δ (‰) relative to the Vienna Peedee Belemnite (VPDB) standard.

Flux partitioning

Mass balance principle

Based on the principle of mass balance, F_A, F_R and their isotopic components can be written after Bowling *et al*. (2001) as

$$F_A + F_R = F_N \tag{1}$$

$$(\delta_a - \Delta_{canopy}) \cdot F_A + \delta_R \cdot F_R = \delta_N \cdot F_N \tag{2}$$

where F_N is directly measured by the EC approach on the assumption that the rate of change of CO_2 storage between the ground and the measurement height is negligible for turbulent conditions (friction velocity $u_* \geq 0.1$ m s^{-1}). A positive sign indicates a flux leaving the surface and a negative sign indicates a flux towards the surface. δ_R and δ_N are the isotope ratios of respired CO_2 and the net exchange of CO_2 between the surface and the atmosphere, respectively. Δ_{canopy} is the whole-canopy photosynthetic discrimination. To solve for F_A and F_R in Eqns 1 and 2, it is necessary to determine the parameters δ_R, Δ_{canopy} and δ_N.

Isotope ratio of ecosystem respiration and net ecosystem CO_2 exchange

δ_R was estimated with the flux ratio method according to Griffis *et al*. (2004b),

$$\frac{F_N^{13}}{F_N^{12}} = \frac{-K_C(\bar{\rho}_a/M_a)\left(d\overline{^{13}CO_2}/dz\right)}{-K_C(\bar{\rho}_a/M_a)\left(d\overline{^{12}CO_2}/dz\right)} \tag{3}$$

where the superscripts 13 and 12 represent $^{13}CO_2$ and $^{12}CO_2$, respectively. K_c is eddy diffusivity, $d\overline{CO_2}/dz$ indicates the time-averaged mixing ratio gradients of $^{13}CO_2$ and $^{12}CO_2$ measured simultaneously at two heights above the canopy and M_a is the molecular weight of dry air. By assuming similarity in the K_C for $^{12}CO_2$ and $^{13}CO_2$, the flux ratio reduces to $d\overline{^{13}CO_2} / d\overline{^{12}CO_2}$, from which δ_R can be derived using night-time data as:

$$\delta_R = \left(\frac{d\overline{^{13}CO_2} / d\overline{^{12}CO_2}}{R_{std}} \right) \times 1000 \quad (4)$$

where R_{std} is the standard molar ratio (see appendix I in Griffis *et al.* 2004b for details). The nightly flux ratio, $d\overline{^{13}CO_2} / d\overline{^{12}CO_2}$, was obtained from the slope of a geometric mean regression between the 2 min measurements of $^{13}CO_2$ and $^{12}CO_2$ made over the entire night. Periods of weak turbulence ($u_* < 0.1$ m s^{-1}) were screened out. For comparison, δ_R was also estimated with the Keeling plot method at the first inlet above the canopy. During the growing season conditions, the flux ratio method cannot estimate daytime δ_R and the Keeling plot method is subject to errors caused by variation of convective boundary layer isotope composition and the influence of photosynthetic activity (Bowling *et al.* 2001; Pataki *et al.* 2003). Therefore, we assumed that the daytime δ_R could be interpolated from two neighbouring night-time periods. This assumption may be violated when there are significant differences in the isotope ratio between the heterotrophic and autotrophic components of respiration.

Similarly, δ_N was estimated with the flux ratio method using 2 min data collected during the daytime. Hourly δ_N values were obtained using measurements made during the previous and the following half-hours and were interpolated into half-hourly values.

Canopy-scale photosynthetic discrimination

By assuming an analogy between the leaf and the canopy-scale photosynthetic discrimination, Δ_{canopy} was determined with the following equations (Farquhar, Ehleringer & Hubick 1989; Bowling *et al.* 2001):

$$-F_A = g_c(C_a - C_i) \quad (5.1)$$

$$\Delta_{canopy} = a + (b_4 + b_3\phi - a)\frac{C_i}{C_a} \quad (5.2)$$

where C_i and C_a are the mixing ratios of the canopy averaged intercellular CO_2 and the ambient CO_2 at the lower inlet above the canopy, respectively. The canopy bulk stomatal conductance for CO_2 (g_c) was inverted from the Penman–Monteith (PM) equation (Appendix I). Parameter a is the discrimination caused by diffusion through the stomata (about 4.4‰), b_3 and b_4 are the discrimination factors related to RuP_2 carboxylation (27‰) and PEP carboxylase (–5.7‰), respectively, and ϕ is the fraction of CO_2 leaking out of the bundle sheath cells and refixed by Rubisco. Literature values of ϕ generally range from 0.2 to 0.5, largely dependent on the anatomical characteristics of leaves and the mesophyll and bundle sheath activities (Hattersley 1982; Evans *et al.* 1986; Farquhar *et al.* 1989). Here, ϕ was constrained from the isotope ratio of top plant leaves (11.8 ± 0.4‰) and Eqn 5.2, which appeared to be approximately 0.3 by assuming a typical C_i/C_a value of 0.3. We assumed that the leaf-scale values of a, b_3, b_4 and ϕ could be applied to the canopy scale (Fung *et al.* 1997; Bowling *et al.* 2001), and obtained the following by rearranging Eqns 5.1 and 5.2:

$$\Delta_{canopy} = a + b' + \frac{b'F_A}{g_c C_a} \quad (5.3)$$

where $b' = b_4 + b_3\phi - a$. δ_R and δ_N were determined directly from measurements. This leaves three unknowns – F_A, F_R and Δ_{canopy} – in the non-linear equation set composed of Eqns 1, 2 and 5.3, allowing an analytical solution. The isotope ratio of the assimilated CO_2 by photosynthesis (δ_P) was derived from $\Delta_{canopy} = (\delta_a - \delta_p) / (1000 + \delta_p)$.

Ecosystem respiration estimated from night-time regression

Ecosystem respiration (R_e) is traditionally estimated with night-time EC data collected under turbulent conditions or with chamber measurements. These data are typically used to develop seasonal or annual relationships between the night-time F_N and soil temperature (T_s) and soil water content (Lloyd & Taylor 1994; Black *et al.* 1996; Lavigne *et al.* 1997; Janssens *et al.* 2001; Barr *et al.* 2002). The night-time F_N showed an exponential relationship with T_s measured at a depth of 2.5 cm. The night-time F_N also increased exponentially with LAI, which was used as a surrogate for the influence of phenology, productivity and increased availability of substrates for respiration. From the foregoing observations, we developed a non-linear regression model for R_e as follows:

$$R_e = A\exp(B_1 T_s + B_2 \mathrm{LAI}) \cdot f(\theta) \quad (6.1)$$

$$f(\theta) = \begin{cases} 2 - \dfrac{\theta}{\theta_0} & \theta \geq 0.24 \\ \dfrac{\theta}{\theta_0} & \theta < 0.24 \end{cases} \quad (6.2)$$

Empirical parameters A, B_1 and B_2 were determined with an optimization method. θ is the volumetric soil water content at 10 cm depth, and θ_0 is the optimal soil water content, which appeared to be 0.24 m^3 m^{-3} for our soil. LAI was simulated with a polynomial regression of measured LAI and time, and T_s and θ were all measured half-hourly. Data collected for $u_* \geq 0.1$ m s^{-1} were used to optimize the parameters A, B_1 and B_2. The regression model explained 66% of the total variance of the measured night-time F_N.

RESULTS AND DISCUSSION

Climate and phenology

The T_s, cumulative precipitation, soil water content and LAI during the growing season are shown in Fig. 1. Soil temperature at the 2.5 cm depth reached a maximum around DOY 166 (Fig. 1a). The summer of 2003 was relatively dry, with only four rain events ≥10 mm. Total precipitation from DOY 121–274 (1 May to 31 September) was 400 mm (Fig. 1b), which was 26% less than the 30-year (1971–2000) climate normal. Soil water content remained relatively low over much of the measurement period (Fig. 1c), ranging from 0.16 to 0.34 m^3 m^{-3}, and generally remained <0.23 m^3 m^{-3} late in the growing season after the

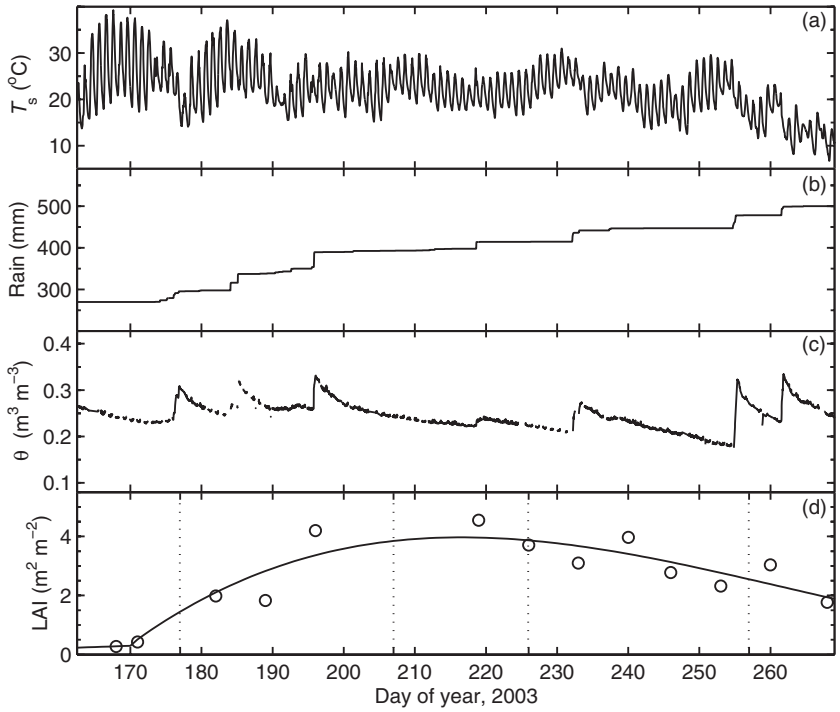

Figure 1. Climate and phenology in 2003: (a) soil temperature at 2.5 cm depth; (b) cumulative precipitation; (c) soil water content at 10 cm depth; and (d) measured leaf area index (LAI) (circles) and simulated LAI (solid line), where the growth stages are indicated by dotted lines.

corn had tasselled. The corn emerged around DOY 135 (15 May) and was harvested on DOY 287 (14 October). The maximum LAI was 4.5 $m^2\ m^{-2}$, observed on DOY 219 (8 August). Critical growth stages (defined in Ritchie, Hanway & Benson 1993) were observed as follows: (1) from emergence to nine-leaf stage (DOY 135–176); (2) from nine-leaf to tassel stage (DOY 177–206), which was the rapid vegetative growth stage; (3) silking and blister (DOY 207–225); and (4) from milk to physiological maturity (DOY 226–257).

Diurnal variation of the CO_2 mixing ratio and carbon isotope ratio of ambient air

Figure 2 shows the ensemble diurnal variation of half-hourly CO_2 mixing ratio and the isotope ratio during typical days (DOY 210–217). The average canopy height was 2.8 m, and the corn canopy had just tasselled. The daytime CO_2 mixing ratio was relatively low, in the vicinity of 350 μmol mol^{-1} (Fig. 2a). The CO_2 mixing ratio began to increase after sunset at around 1900 h and reached a max-

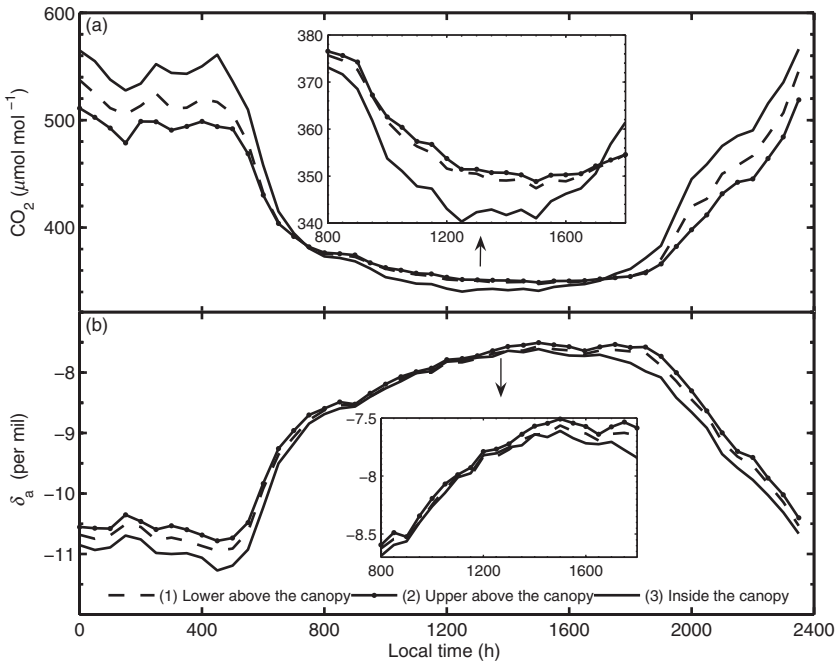

Figure 2. Ensemble diurnal variations of CO_2 mixing ratio and isotope ratio during day of year (DOY) 210–217 (29 July to 5 August). (a) mixing ratios of CO_2 at three heights, two above the canopy and one inside the canopy; and (b) isotope ratios of ambient air at the three heights. Daytime details are shown in the magnified inset figures.

imum at midnight. The range of daytime CO_2 mixing ratio was small, typically less than 40 μmol mol^{-1}, while the range at night was often greater than 100 μmol mol^{-1}.

The effects of photosynthesis and respiration on atmospheric $^{13}CO_2$ abundance were also indicated in the temporal variation of the isotope ratio (Fig. 2b). During the daytime, air was enriched in $^{13}CO_2$ because of photosynthetic discrimination, and the isotope ratio was relatively high, about –7.6‰. At night, the values were more negative as a result of respiration and were typically around –10.6‰. Similar diurnal patterns of CO_2 mixing ratio and isotope ratio were observed by Buchmann & Ehleringer (1998) over a corn canopy.

The differences in CO_2 mixing ratio and isotope ratio among the three measurement heights were most evident at night. During the day, the differences were relatively small but significant (i.e. greater than the measurement precision of the TDL, see Griffis *et al*. 2004b). The inlet inside the canopy (1.0 m from the ground) typically measured the lowest CO_2 mixing ratio and the most negative isotope ratio. The daytime relative depletion of $^{13}CO_2$ inside the canopy was most likely a result of ecosystem respiration. Light attenuation may also cause $^{13}CO_2$ depletion through increasing C_i/C_a (and thus photosynthetic discrimination). However, this effect is estimated to be small for C_4 plants according to Eqn 5.3 and Farquhar *et al*. (1989).

Canopy bulk stomatal conductance for CO_2

The determination of g_c is critical to flux partitioning because it is directly related to the photosynthetic computation (Eqn 5). Unfortunately, the g_c estimated with the PM equation can involve relatively large uncertainties resulting from lack of energy balance closure, the generally unknown contribution of soil evaporation and errors associated with EC measurements. To limit these problems, we forced energy balance closure using the Bowen ratio obtained from the EC measurements (Twine *et al*. 2000), and limited our analysis to turbulent conditions when the canopy was dry (83% of the data). During the full canopy period (LAI ≥ 2), soil evaporation accounted for 3–10% of the total canopy evapotranspiration, leading to an overestimation of 1.2–12% of g_c (Appendix II). The uncertainty in g_c, caused by measurement errors in H, λE, wind speed (u) and water vapour pressure deficit (VPD) was estimated to be approximately 30% (see Appendix II for the details of uncertainty analysis).

Figure 3 shows the ensemble diurnal variations of g_c. Maximum g_c was observed during the rapid vegetative growth stage (Fig. 3a), about 0.5 mol m^{-2} s^{-1}. Late in the growing season, g_c decreased to less than 0.2 mol m^{-2} s^{-1} (Fig. 3c). These values are in good agreement with other studies (Kelliher *et al*. 1995; Steduto & Hsiao 1998). For most of the experimental period, the daily maximum g_c tended to skew towards the morning, which is typical for a canopy that is water stressed (Steduto & Hsiao 1998; Kurpius *et al*. 2003).

Isotope ratio of ecosystem respiration

The uncertainties in the flux ratio and Keeling estimates of nightly δ_R using 2 min data collected over the entire night are shown in Table 1. The uncertainty of the flux ratio estimate was typically 0.7‰, which was larger than the Keeling estimate of about 0.4‰. The uncertainties of both methods increased significantly as the range of CO_2 mixing ratio decreased, an occurrence that has also been reported in other studies (Pataki *et al*. 2003). For instance, to limit the

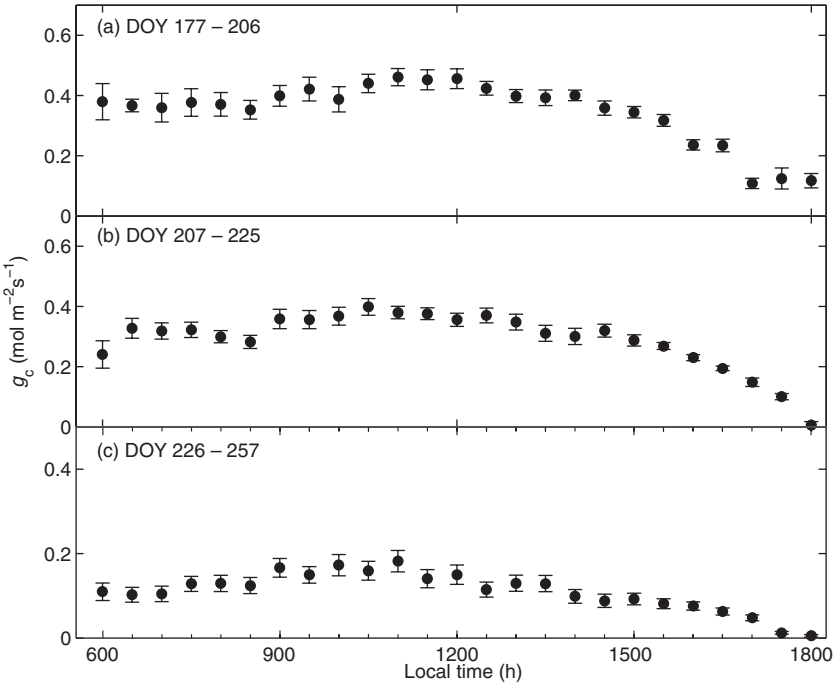

Figure 3. Ensemble diurnal variation of g_c during critical growth stages. Error bars represent the standard error of the mean.

Table 1. The uncertainties in the estimation of nightly δ_R. The uncertainty of the Keeling estimate is the standard error of the intercept. The uncertainty of the flux ratio estimate is calculated as (standard error of the slope / R_{std}) × 1000 (‰). Two-minute data collected over the entire night when $u_* \geq 0.1$ m s^{-1} were used for both methods

Statistics	Flux ratio	Keeling intercept	Units
r^2	> 0.99	0.8	–
Standard error	0.7	0.4	‰
CO_2 range	40[a]	102	μmol mol^{-1}

[a]The range of the difference in CO_2 mixing ratio between the two intakes above the canopy.

uncertainty to within 3‰, the Keeling method required ≥ 10 μmol mol^{-1} range of CO_2 mixing ratio (about 99% of the night-time observations met this threshold), and the flux ratio method required ≥ 10 μmol mol^{-1} range of CO_2 mixing ratio difference between the two inlets (about 92% of the night-time observations met this threshold).

Night-time hourly δ_R obtained with the flux ratio method showed considerable variations, with values typically fluctuating by about 2.0‰. Bowling *et al*. (2003) also reported significant hourly variation of up to 6.4‰ for δ_R in a grassland. For a typical nocturnal pattern, hourly δ_R values decreased with time and reached a minimum value before sunrise. There are two possible explanations for this observation. Firstly, the isotopic composition of rhizosphere respiration may have become more depleted during the night as the substrates that were assimilated during the daytime were consumed and microbes switched to other available substrates that were less enriched. Secondly, as the night progressed, the above-ground foliar respiration could have been inhibited more than the below-ground heterotrophic respiration as a result of decreasing air temperature or substrate availability. Both mechanisms could cause δ_R to become relatively more depleted over the course of the night. The considerable hourly variation of night-time δ_R implies that there might be important limitation on the extrapolation of night-time δ_R to daytime values in the isotopic flux partitioning. Daytime chamber measurements on the individual component of ecosystem respiration are needed to examine this issue in further detail.

The flux ratio and the Keeling estimates of nightly δ_R are shown in Fig. 4. On average, the Keeling method tended to give lower values particularly during the full canopy closure period (LAI ≥ 2, DOY 177–257). One possible explanation for the discrepancy is the fetch mismatch between the two methods. A footprint analysis (Schuepp *et al*. 1990) showed that the effective fetch of the mixing ratio measurement at night was typically > 270 m, which was larger than the 200 m fetch of the site. It is possible that the advection of depleted CO_2 from the surrounding C_3 vegetation (forests and some agricultural crops) and combustion sources had influenced the mixing ratio measurements, resulting in lower Keeling estimates. In comparison, the flux measurement (derived from mixing ratio gradient) typically had an effective fetch of less than 150 m, implying that the influence of advection on the flux ratio method was smaller.

Another possible reason for the difference is the variation of boundary layer atmospheric CO_2. As CO_2 is respired and mixed into the nocturnal boundary layer, the mixing ratio and the isotope ratio of 'background CO_2' ($C_{bg} = C_a - C_R$, where C_R is the mixing ratio of respired CO_2) varies over the course of the night. In addition, it is possible that advection from C_3 vegetation or combustion sources could have affected the 'background CO_2' considerably. This temporal variation of boundary layer CO_2 introduces a bias into the night-time Keeling estimates. We hypothesized that at an hourly timescale the changes in the nocturnal boundary layer characteristics are smaller and have less influence on the Keeling estimates. We observed that the nightly Keeling estimates were generally 2‰ lower than the hourly values averaged over the entire night (hourly estimates with a standard error of σ < 1‰ were used). The flux ratio estimates did not show such significant difference between the hourly and nightly values. For hourly δ_R values, the flux ratio and the Keeling methods showed a typical difference of 1.7‰, which is smaller than the 3.5‰ difference for nightly values. At this point, the influence of background CO_2 variation on the Keeling estimates cannot be evaluated directly. Boundary layer modelling is needed to explore this issue in greater detail. Taking into account the possible influence of advection and background CO_2 on the Keeling plot and to be consistent in terms of footprint match with F_N and δ_N, we used the flux ratio method for nightly δ_R in the following partitioning.

Considerable seasonal variation in night-time δ_R was observed (Fig. 4). During the spring (DOY < 160), values fluctuated between approximately –32 and –19‰, and then increased rapidly to a maximum of approximately –11‰ in early August (around DOY 214) before declining in the fall (> DOY 255) to values in the range of –32 to –20‰. This seasonal variation of δ_R was strongly related to the canopy development, as indicated by a linear relationship with LAI ($r^2 = 0.64$, $P < 0.001$). We hypothesized that the higher values during DOY 182–243 (July to August) were largely attributable to the increase in the more enriched autotrophic respiration of the C_4 corn. Lai *et al*. (2003) has also reported impacts of phenology on seasonal variation of δ_R over a mixed C_4–C_3 grassland, where δ_R did not show distinct temporal pattern because of the changes in C_3 and C_4 contributions. The rapid decline in δ_R at the conclusion of the growing season was somewhat unexpected. However, during this period (DOY 255–263), a rain event increased the θ from 0.2 to 0.25 m^3 m^{-3}. Soil temperature at 2.5 cm depth also increased from 10 to > 20 °C (data not shown). The relatively warm, moist conditions likely stimulated heterotrophic respiration, causing a decrease in δ_R.

δ_R has also been shown to be influenced by precipitation, soil water content and VPD (Ehleringer & Cerling 1995; Bowling *et al*. 2002; Ometto *et al*. 2002; Fessenden & Ehleringer 2003; Lai *et al*. 2004; McDowell *et al*. 2004), which could explain some of the large day-to-day variations

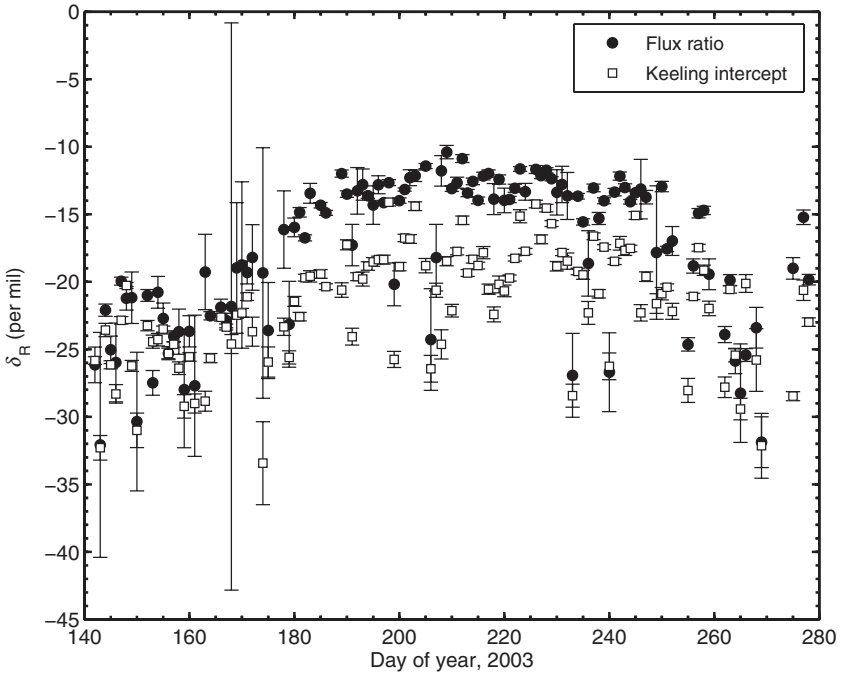

Figure 4. Seasonal variation of δ_R in 2003. Error bars indicate the uncertainties (standard errors) of the flux ratio and Keeling estimates, respectively.

in δ_R. For instance, the abnormally low values of δ_R on DOY 235, 255 and 262 were preceded by rain events within 48 h. However, the low values of δ_R on DOY 190 and 198 were not related to θ or precipitation. Those days were characterized by low air temperature and low solar radiation, both of which would be expected to have a greater negative impact on the above-ground foliar respiration than the below-ground heterotrophic respiration. In addition, the reduced carbon assimilation, partly reflected in the low F_N values, might also limit autotrophic respiration.

Isotope ratio of net ecosystem CO_2 exchange and photosynthetic discrimination

Figure 5 shows the ensemble δ_R and δ_N estimated with the flux ratio method. The figure also shows Δ_{canopy} and the isotopic ratio of the canopy photosynthesis (δ_P) obtained after F_A was partitioned. δ_N depends on the magnitude of F_N, δ_R and Δ_{canopy}. It is therefore not surprising that relatively large fluctuations were observed in δ_N. For the majority of the daytime values, δ_N varied between –12 and –4‰. The Δ_{canopy} remained relatively constant both diurnally and seasonally in the vicinity of 3‰, which was smaller than the value of approximately 4‰ deduced from the difference between the measured plant isotope ratio (top leaves -11.8 ± 0.4‰, bottom leaves -12.3 ± 0.3‰) and the mean ambient air ratio of –7.8‰. The relatively constant Δ_{canopy} resulted from the positive contribution of PEP carboxylase to the assimilation of $^{13}CO_2$, about –5.7‰ in terms of discrimination.

The Δ_{canopy} is an important factor in some biophysical models (e.g. SiB2) that are used to partition the carbon budget at the global scale (Ciais *et al*. 1995; Fung *et al*. 1997). Fung *et al*. (1997) showed that a change of 3‰ in annual mean Δ_{canopy} could cause a 0.7 Gt C year^{-1} bias in the carbon sink. Here, the estimate of Δ_{canopy} is smaller than the global mean value of 3.6‰ for C_4 plants reported by Lloyd & Farquhar (1994). While the Δ_{canopy} remained relatively stable in our study, the Δ_{canopy} of C_3 or mixed C_4–C_3 ecosystems typically shows significant diurnal and seasonal variations resulting from changes in C_i/C_a. Lai *et al*. (2003) observed an apparent diurnal pattern of Δ_{canopy} ranging from about 0.7‰ in the morning and evening to approximately 2.8‰ at midday over a mixed C_4–C_3 grassland. Bowling *et al*. (2001) also observed a strong diurnal variation of Δ_{canopy}, approximately 16 to 19‰ over a temperate deciduous forest.

Partitioning net ecosystem CO_2 exchange into photosynthesis and respiration

Half-hourly F_N was partitioned into photosynthesis and respiration using both the isotopic approach and the regression method for the full canopy period. The diurnal ensemble partitioning for each growth stage is shown in Fig. 6. In general, F_A ranged between –30 and –50 μmol m^{-2} s^{-1}, and F_R typically varied from slightly above zero to 15 μmol m^{-2} s^{-1}. These results are consistent with other values in literature (Grant *et al*. 1989; Pattey *et al*. 1991; Steduto & Hsiao 1998). Both F_A and F_R peaked during the silking to blister stage (DOY 207–225) (Fig. 6b). The isotopic flux partitioning generally showed larger half-hourly variability than the regression method. The differences between the two methods were particularly significant at around midday, when F_R sometimes showed depressions while R_e continued to increase with time. No significant relationship between R_e and F_R was observed from 1:1 plots (figures not shown).

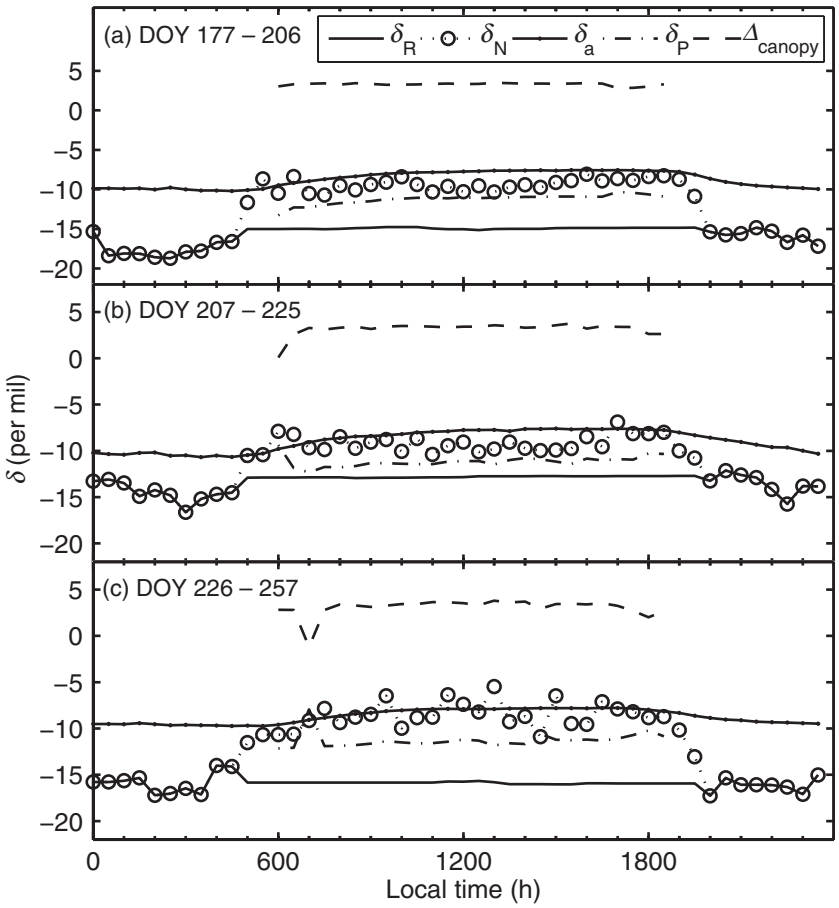

Figure 5. Ensemble diurnal variations of δ_R (solid line), δ_N (dotted line with circles), δ_P (dot-dashed line), δ_a (solid line with points) and Δ_{canopy} (dashed line).

We note that the daytime pattern of R_e is a direct consequence of the soil temperature and water content changes and might not represent the true physiological response of the ecosystem. Studies suggest that the night-time regression method might considerably overestimate the daytime respiration by up to 15% without considering the photoinhibition effect of photosynthesis on foliar respiration (Kok effect) (Brooks & Farquhar 1985; Janssens *et al*. 2001). The values of F_R, however, were sometimes unrealistically low during midday (Fig. 6a & b). This might be related to the uncertainties associated with the TDL and micrometeorological measurements (discussed in further detail below). It is also important to note, however, that the isotopic flux partitioning based on mass balance principle might have considerably underestimated the photosynthesis and respiration without considering the process of CO_2 recycling inside the canopy (Greaver *et al*. 2005).

Uncertainty analysis of isotopic flux partitioning and future recommendations

Unrealistic isotopic partitioning, that is, unrealistic values of F_R, were observed, indicating that there are important uncertainties in the micrometeorological-stable isotope technique that require further investigation. For example, at around 1130 h in Fig. 6b and 1230 h in Fig. 6c, the partitioned F_R was apparently below zero. In addition, the particularly high values of F_R, about 15 μmol m^{-2} s^{-1}, at around 1200 and 1300 h shown in Fig. 6c were unreasonable for the late growing season. These failed cases were usually associated with very low δ_N values, high daytime δ_R values, or in some cases, the unreasonably high or low g_c values, assuming F_N to be the 'true' value. Considering the magnitude of errors typically involved in the half-hourly micrometeorological measurement, which could be up to 30%, and the uncertainties in the half-hourly TDL values of δ_N and δ_R, we should not be surprised by the relatively large errors in the isotopic flux partitioning.

The total uncertainty in the partitioning of F_A, propagated from errors of individual variables, was calculated according to Bevington (1969) (see Appendix II for the details of error propagation). Results showed that the total uncertainty was typically around 30% in the early growth season and increased to > 40% for the mid and late seasons when the difference between the isotope ratio of photosynthesis and respiration was small or otherwise the fluxes were small. An uncertainty test was therefore performed to examine the contribution of each variable to the total uncertainty. In order to identify the influence of isotopic disequlibrium or $|\delta_R - \delta_P|$, we selected the early and mid seasons as two examples for which the mean δ_R was assigned to be –20 and –14‰, respectively. The mean values and uncertainties of C_a, g_c, δ_N and δ_a were assigned constant values (Table 2). The individual contributions are shown in

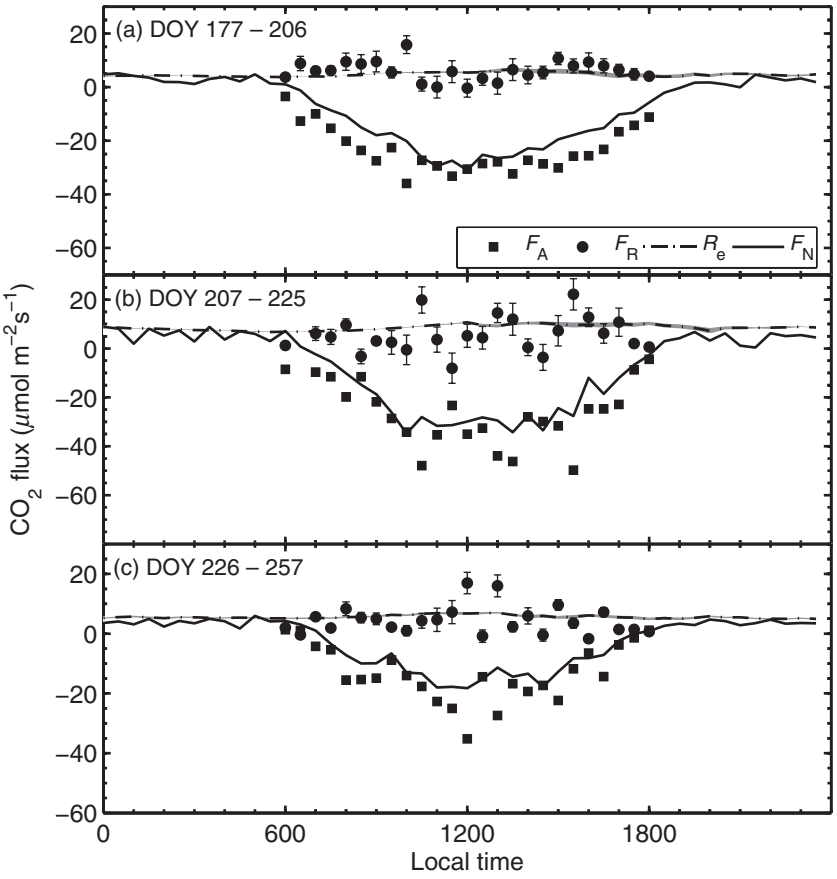

Figure 6. Ensemble diurnal variations of photosynthesis and respiration from the isotopic partitioning method and night-time regression method during critical growth stages. The shaded area and error bars indicate the standard error of R_e and F_R, respectively.

Table 3, which also shows the partial derivatives evaluated at the mean values. These partial derivatives indicate the sensitivity of F_A to each variable.

The results indicated that the uncertainties in δ_N estimates imposed the most significant influence on the partitioning, accounting for more than 80% of the total uncertainty (Table 3). The partitioning was also highly sensitive to δ_N, with a 1‰ fluctuation in δ_N resulting in a 10 and 25% change of F_A for the early and mid season, respectively. As reported in other studies, the precise estimation of δ_N (or isoflux $\delta_N \cdot F_N$) is essential to the isotopic flux partitioning (Bowling *et al*. 2001; Lai *et al*. 2003; Ogée *et al*. 2003, 2004). In this study, the uncertainty in the hourly flux ratio estimate of δ_N was large, ranging from 0.5 to 6‰ because of the relatively small differences in the CO_2 mixing ratios between the two inlets during the daytime (< 1.5 μmol mol^{-1}). The precision of δ_N could be improved by increasing the separation between the two measuring levels to obtain larger gradients in $^{12}CO_2$ and $^{13}CO_2$ or by extending the sampling period. Buffer volumes could be used to reduce the noise caused by turbulent fluctuations in the TDL measurements of $^{12}CO_2$ and $^{13}CO_2$. The uncertainty in F_A could also be reduced by measuring the flux of $^{13}CO_2$ directly with EC, by which the problems related to footprint mismatch and small gradient on the isoflux estimation would be overcome. For instance, the total uncertainty in F_A will decrease by approximately 50% for both the early and mid growing seasons (according to the values in Table 2 and by considering $\delta_N \times F_N$ as a single variable), if the assumption of 20% error for the $^{13}CO_2$ flux measurement is made.

The fluctuation in δ_R also contributed considerably, though much less than δ_N, to the total uncertainty (Table 3). The uncertainty in δ_R accounted for approximately 17% during the mid season when the isotopic disequlibrium was small (≈ 3‰), and about 2% early in the growing season when the disequilibrium was large (≈ 9‰). Based on the sensitivity of the partitioning to δ_R [$\left|\left.\frac{\partial F_A}{\partial \delta_R}\right|_{x_0} / F_A \times 100(\%)\right|$ in

Table 2. The means and uncertainties of the individual variables used in the uncertainty test. The uncertainties of C_a and δ_a are the measurement precisions of tunable diode laser (TDL) (Griffis *et al*. 2004b). The uncertainty of δ_N is the standard error of the flux ratio estimate. The uncertainty of δ_R is the hour-to-hour variability of night-time values

Variable	Mean values	Uncertainties	Units
δ_a	–7.5	0.07	‰
δ_N	–9	3	‰
δ_R	–20/–14[a]	2	‰
g_c	0.3	0.09	mol m^{-2} s^{-1}
C_a	350	0.03	μmol mol^{-1}
F_N	–25	0[b]	μmol m^{-2} s^{-1}

[a]Mean values of δ_R in early/mid growing seasons.
[b]F_N was assumed to be the 'true' value.

Table 3. Contributions of individual variables to the total uncertainty in F_A. p_i represents the contribution of individual variable x_i to the total uncertainty. The typical mean value x_0 and the uncertainty of each variable are given in Table 2

	Early season		Mid season	
Variable x_i	p_i (%)	$\left\|\frac{\partial F_A}{\partial x_i}\right\|_{x0} / F_A \times 100(\%)$	p_i (%)	$\left\|\frac{\partial F_A}{\partial x_i}\right\|_{x0} / F_A \times 100(\%)$
δ_a	0.1	11.5	0.1	41.8
δ_N	97.8	9.5	82.2	24.9
δ_R	1.8	1.9	16.9	17.1
g_c	0.2	16.0	0.8	81.3
C_a	< 0.01	< 0.01	< 0.01	< 0.01

Table 3], the 2‰ difference between the hourly flux ratio and the Keeling estimates of δ_R resulted in an approximate 4% change in F_A in the early season and up to > 30% variation in the mid season when the isotopic disequilibrium was relatively small.

The g_c estimate was expected to involve large uncertainties (see Appendix II). However, the contribution of g_c errors to the total uncertainty varied considerably with the errors of other variables. For instance, the error in g_c accounted for less than 1% of the total uncertainty when the uncertainties of δ_R and δ_N were relatively large (i.e. > 2‰). The error in g_c accounted for more than 25% when the uncertainty of δ_R and δ_N was limited to within 0.5‰.

The influence of isotopic disequilibrium on flux partitioning is significant because the methodology will fail if δ_P equilibrates with δ_R. Ogée *et al*. (2004) showed that a small disequilibrium between δ_P and δ_R resulted in large uncertainties in the partitioning even after the precision of δ_R and δ_N was improved. Our results showed that the isotopic partitioning produced better results (indicated by less negative F_R values) before DOY 185 when the difference between δ_P and δ_R was relatively large (> 5‰). According to the uncertainty analysis, the total uncertainty in F_A increased from ≈ 30 to > 40% when $|\delta_R - \delta_P|$ decreased from ≈ 9‰ in the early season to ≈ 3‰ in the mid season.

Although the partitioning showed high sensitivity to δ_a (Table 3), the instrumental errors in δ_a measurements are typically small and have a small influence (less than 0.1%) on the partitioning. The uncertainties associated with parameters a, b_3 and b_4 require further investigation and were not explicitly considered here. Nevertheless, the partitioning appears to be highly sensitive to these parameters. For instance, if the value of b_3 is changed from 27 to 29‰, the F_A would be altered by about 10% on average for all seasons. In addition, it is unlikely that ϕ will remain constant for different varieties of corn or for different environmental conditions. The assumption of the analogy between the leaf-scale and the canopy-scale discrimination needs further investigation. Leaf-scale measurements of isotopic exchange, stomatal conductance and photosynthesis, combined with physiological modelling, could provide additional insight into these issues.

CONCLUSIONS

In this study, TDL measurements of $^{12}CO_2$ and $^{13}CO_2$ mixing ratios were combined with micrometeorological techniques to partition the net ecosystem CO_2 exchange of a C_3–C_4 rotation agricultural ecosystem into photosynthesis and respiration on a half-hourly basis. We conclude that:

1 The ecosystem respiration partitioned with isotopic flux approach typically varied from about 0 to 15 μmol m^{-2} s^{-1} and the photosynthesis varied from about 30 to 50 μmol m^{-2} s^{-1} during the full canopy period. The isotopic approach generally showed greater variability than the night-time regression method and tended to give lower, and sometimes unrealistic, midday values.

2 The isotope ratio of night-time respiration showed significant seasonal variation from –32 to –11‰, corresponding with the seasonal development of the canopy. Night-time hourly variations of typically 2‰ were also observed. Therefore, the extrapolation of night-time values to the daytime represents a potentially important limitation to the isotopic flux partitioning methodology. The whole canopy photosynthetic discrimination remained relatively constant both diurnally and seasonally in the vicinity of 3‰. The isotope ratio of net CO_2 exchange showed significant hour-to-hour variation within the range of –12 to –4‰.

3 The uncertainty in the isotopic flux partitioning methodology varied seasonally and diurnally. The largest source of uncertainty was related to the estimation of the isotope ratio of net CO_2 exchange, or alternatively, the isoflux estimation. The isotopic flux partitioning could be considerably improved if the $^{13}CO_2$ flux were measured directly using the EC technique. Furthermore, uncertainty in the isotopic partitioning was significantly reduced when the isotopic disequilibrium exceeded 5‰, which was observed at this site during the early growing season.

4 We expect that the isotopic flux partitioning approach could be greatly improved if the uncertainty in the flux ratio estimate of net ecosystem CO_2 exchange was substantially reduced. We believe there is an opportunity to achieve this through the combination of the TDL and EC approach.

ACKNOWLEDGMENTS

This research was supported by the Office of Science (BER), US Department of Energy, grant No. DE-FG02-03ER63684, and the University of Minnesota, Grant-in-Aid-of-Research, Artistry and Scholarship Program (TJG). The authors would like to thank the two anonymous reviewers and Dr Scott Saleska at the University of Arizona for their critical and constructive comments. We appreciate the field assistance of W.A. Breiter and K. Vang. Finally, we gratefully acknowledge the logistical support provided by the University of Minnesota, Rosemount Research and Outreach Center and the USDA-ARS.

REFERENCES

Baker J.M. & Griffis T.J. (2005) Examining strategies to improve the carbon balance of corn/soybean agriculture using eddy covariance and mass balance techniques. *Agricultural and Forest Meteorology* **128,** 163–177.

Baldocchi D.D. & Harley P.C. (1995) Scaling carbon dioxide and water vapor exchange from leaf to canopy in a deciduous forest. II. Model testing and application. *Plant, Cell and Environment* **18,** 1157–1173.

Barr A.G., Griffis T.J., Black T.A., Lee X., Staebler R.M., Fuentes J.D., Chen Z. & Morgenstern K. (2002) Comparing the carbon budgets of boreal and temperate deciduous forest stands. *Canadian Journal of Forest Research* **32,** 813–822.

Battle M., Bender M.L., Tans P.P., White J.W.C., Ellis J.E., Conway T. & Francey R.J. (2000) Global carbon sinks and their variability inferred from atmospheric O_2 and $\delta^{13}C$. *Science* **287,** 2467–2470.

Bevington P.R. (1969) *Data Reduction and Error Analysis for the Physical Science.* McGraw-Hill Book company, New York, USA.

Black T.A., DenHartog G., Neumann H.H., *et al.* (1996) Annual cycles of water vapor and carbon dioxide fluxes in and above a boreal aspen forest. *Global Change Biology* **2,** 219–229.

Bowling D.R., Tans P.P. & Monson R.K. (2001) Partitioning net ecosystem carbon exchange with isotopic fluxes of CO_2. *Global Change Biology* **7,** 127–145.

Bowling D.R., McDowell N.G., Bond B.J., Law B.E. & Ehleringer J.R. (2002) ^{13}C content of ecosystem respiration is linked to precipitation and vapor pressure deficit. *Oecologia* **131,** 113–124.

Bowling D.R., Sargent S.D., Tanner B.D. & Ehleringer J.R. (2003) Tunable diode laser absorption spectroscopy for stable isotope studies of ecosystem–atmosphere CO_2 exchange. *Agricultural and Forest Meteorology* **118,** 1–19.

Brooks A. & Farquhar G.D. (1985) Effects of temperature on the CO_2/O_2 specificity of ribulose-1, 5-bisphosphate carboxylase/oxygenase and the rate of respiration in the light. *Planta* **165,** 397–406.

Buchmann N. & Ehleringer J.R. (1998) CO_2 mixing ratio profiles, and carbon and oxygen isotopes in C_3 and C_4 crop canopies. *Agricultural and Forest Meteorology* **89,** 45–58.

Ciais P., Tans P.P., Trolier M., *et al.* (1995) Partitioning of ocean and land uptake of CO_2 as inferred by $\delta^{13}C$ measurements from the NOAA Climate Monitoring and Diagnostics Laboratory Global Air Sampling Network. *Journal of Geophysical Research-Atmospheres* **100,** 5051–5070.

Drewitt G.B., Black T.A., Nesic Z., Humphreys E.R., Jork E.M., Swanson R., Ethier G.J., Griffis T.J. & Morgenstern K. (2002) Measuring forest floor CO_2 fluxes in a Douglas-fir forest. *Agricultural and Forest Meteorology* **110,** 299–317.

Ehleringer J.R. & Cerling T.T. (1995) Atmospheric CO_2 and the ratio of intercellular to ambient CO_2 concentrations in plants. *Tree Physiology* **15,** 105–111.

Evans J.R., Sharkey T.D., Berry J.A. & Farquhar G.D. (1986) Carbon isotope discrimination measured concurrently with gas exchange to investigate CO_2 diffusion in leaves of higher plants. *Australian Journal of Plant Physiology* **13,** 281–292.

Falge E., Baldocchi D.D., Tenhunen J., Aubinet M., Bakwin P., Berbigier P., Bernhofer C., Burba G., Clement R. & Davis K.J. (2002) Seasonality of ecosystem respiration and gross primary production as derived from FLUXNET measurements. *Agricultural and Forest Meteorology* **113,** 53–74.

Farquhar G.D., Ehleringer J.R. & Hubick K.T. (1989) Carbon isotope discrimination and photosynthesis. *Annual Review of Plant Physiology and Plant Molecular Biology* **40,** 503–537.

Fessenden J.E. & Ehleringer J.R. (2003) Temporal variation in $\delta^{13}C$ of ecosystem respiration in the Pacific Northwest: links to moisture stress. *Oecologia* **136,** 129–136.

Flanagan L.B. & Ehleringer J.R. (1997) Ecosystem-atmosphere CO_2 exchange: interpreting signals of change using stable isotope ratios. *Trends in Ecology and Evolution* **13,** 10–14.

Fung I., Field C.B., Berry J.A., *et al.* (1997) Carbon 13 exchanges between the atmosphere and biosphere. *Global Biogeochemical Cycles* **11,** 507–533.

Goulden M.L., Daube B.C., Fan S.-M., Sutton D.J., Bazzaz A., Munger J.W. & Wofsy S.C. (1997) Physiological responses of a black spruce forest to weather. *Journal of Geophysical Research-Atmospheres* **102,** 28987–28996.

Grant R.R., Peters D.B., Larson E.M. & Huck M.G. (1989) Simulation of canopy photosynthesis in maize and soybean. *Agricultural and Forest Meteorology* **48,** 75–92.

Greaver T., Sternberg L., Schaffer B. & Moreno T. (2005) An empirical method of measuring CO_2 recycling by isotopic enrichment of respired CO_2. *Agricultural and Forest Meteorology* **128,** 67–79.

Griffis T.J., Black T.A., Morgenstern K., Barr A.G., Nesic Z., Drewitt G.B., Gaumont-Guay D. & McCaughey H. (2003) Ecophysiological controls on the carbon balances of three southern boreal forests. *Agricultural and Forest Meteorology* **117,** 53–71.

Griffis T.J., Black T.A., Gaumont-Guay D., Drewitt G.B., Nesic Z., Barr A.G., Morgenstern K. & Kljun N. (2004a) Seasonal variation and partitioning of ecosystem respiration in a southern boreal aspen forest. *Agricultural and Forest Meteorology* **125,** 207–223.

Griffis T.J., Baker J.M., Sargent S.D., Tanner B.D. & Zhang J. (2004b) Measuring field-scale isotopic CO_2 fluxes with tunable diode laser absorption spectroscopy and micrometeorological techniques. *Agricultural and Forest Meteorology* **124,** 15–29.

Griffis T.J., Baker J.M. & Zhang J. (2005) Seasonal dynamics and partitioning of isotopic CO_2 exchange in a C_3/C_4 managed ecosystem. *Agricultural and Forest Meteorology* **132,** 1–19.

Hanson P.J., Edwards N.T., Garten C.T. & Andrews J.A. (2000) Separating root and soil microbial contributions to soil respiration: a review of methods and observations. *Biogeochemistry* **48,** 115–146.

Hattersley P.W. (1982) $\delta^{13}C$ values of C_4 types in grasses. *Australian Journal of Plant Physiology* **9,** 139–154.

Janssens I.A., Lankreijer H., Matteucci G., *et al.* (2001) Productivity overshadows temperature in determining soil and ecosystem respiration across European forests. *Global Change Biology* **7,** 269–278.

Keeling C.D. (1958) The mixing ratio and isotopic abundances of atmospheric carbon dioxide in rural areas. *Geochimica et Cosmochimica Acta* **13,** 322–334.

Kelliher F.M., Leuning R., Raupach M.R. & Schulze E.D. (1995)

Maximum conductances for evaporation from global vegetation types. *Agricultural and Forest Meteorology* **73,** 1–16.

Kurpius M.R., Panek J.A., Nikolov N.T., Mckay M. & Goldstein A.H. (2003) Partitioning of water flux in a Sierra Nevada ponderous pine plantation. *Agricultural and Forest Meteorology* **117,** 173–192.

Lai C.-T., Schauer A.J., Owensby C., Ham J.M. & Ehleringer J.R. (2003) Isotopic air sampling in a tall grass prairie to partition net ecosystem CO_2 exchange. *Journal of Geophysical Research-Atmospheres* **108,** 4566, 10.1029/2002JD003369.

Lai C.-T., Ehleringer J.R., Tans P., Wofsy S.C., Urbanski S.P. & Hollinger D. (2004) Estimating photosynthetic ^{13}C discrimination in terrestrial CO_2 exchange from canopy to regional scales. *Global Biogeochemical Cycles* **18,** GB1041. doi: 10.1029/2003GB002148.

Lavigne M.B., Ryan M.G., Anderson D.E., *et al.* (1997) Comparing nocturnal eddy covariance measurements to estimates of ecosystem respiration made by scaling chamber measurements and six coniferous boreal sites. *Journal of Geophysical Research-Atmospheres* **102,** 28 977–28 928, 28 985.

Lloyd J. & Farquhar G.D. (1994) ^{13}C discrimination during CO_2 assimilation by the terrestrial biosphere. *Oecologia* **99,** 201–215.

Lloyd J. & Taylor J.A. (1994) On the temperature dependence of soil respiration. *Functional Ecology* **8,** 315–323.

Lloyd J., Krujit B. & Hollinger D.Y. (1996) Vegetation effects on the isotopic composition of atmospheric CO_2 at local and regional scales: theoretical aspects and a comparison between rain forest in Amazonia and a boreal forest in Siberia. *Australian Journal of Plant Physiology* **23,** 371–399.

McDowell N.G., Bowling R., Bond B.J., Irvine J., Law B.E., Anthoni P. & Ehleringer J.R. (2004) Response of the carbon isotopic content of ecosystem, leaf, and soil respiration to meteorological and physiological driving factors in a *Pinus ponderosa* ecosystem. *Global Biogeochemical Cycles* **18,** GB1013, doi: 10.1029/2003GB002049.

Morgenstern K., Black T.A., Humphreys E.R., Griffis T.J., Drewitt G.B., Cai T., Nesic Z., Spittlehouse D.L. & Livingston N.J. (2004) Sensitivity and uncertainty of the carbon balance of a Pacific Northwest Douglas-fir forest during an El Niño/La Niña cycle. *Agricultural and Forest Meteorology* **123,** 201–219.

Ogée J.P., Peylin P., Ciais P., Bariac T., Brunet Y., Berbigier P., Roche C., Richard P., Bardoux G. & Bonnefond J.-M. (2003) Partitioning net ecosystem carbon exchange into net assimilation and respiration using $^{13}CO_2$ measurements: a cost-effective sampling strategy. *Global Biogeochemical Cycles* **17,** 1070, doi: 10.1029/2002GB001995.

Ogée J.P., Peylin P., Cuntz M., Bariac T., Brunet Y., Berbigier P., Richard P. & Ciais P. (2004) Partitioning net ecosystem carbon exchange into net assimilation and respiration with canopy-scale isotopic measurements: an error propagation analysis with $^{13}CO_2$ and $CO^{18}O$ data. *Global Biogeochemical Cycles* **18,** GB2019, doi: 10.1029/2003GB002166.

Ometto J.P.H.B., Flanagan L.B., Martinelli L.A., Moreira M.Z., Higuchi N. & Ehleringer J.R. (2002) Carbon isotope discrimination in forest and pasture ecosystems of the Amazon Basin, Brazil. *Global Biogeochemical Cycles* **16,** 1109, doi: 10.1029/2001GB001462.

Owen P.R. & Thomson W.R. (1963) Heat transfer across rough surfaces. *Journal of Fluid Dynamics* **15,** 321–334.

Pataki D.E., Ehleringer J.R., Flanagan L.B., Yakir D., Bowling D.R., Still C.J., Buchmann N., Kaplan J.O. & Berry J.A. (2003) The application and interpretation of Keeling plots in terrestrial carbon cycle research. *Global Biogeochemical Cycles* **17,** 1022, doi: 10.1029/2001GB001850.

Pattey E., Rochette P., Desjardins R.L. & Dubé P.A. (1991) Estimation of the net CO_2 assimilation rate of a maize (*Zea mays* L.) canopy from leaf chamber measurements. *Agricultural and Forest Meteorology* **55,** 7–57.

Price D.T. & Black T.A. (1990) Effects of short-term variation in weather on diurnal canopy CO_2 flux and evapotranspiration of a juvenile Douglas-fir stand. *Agricultural and Forest Meteorology* **50,** 139–158.

Ritchie S.W., Hanway J.J. & Benson G.O. (1993) How a corn plant develops. Iowa State University Cooperative Extension Service, Special Report no. 48.

Rochette P., Flanagan L.B. & Gregorich E.G. (1999) Separating soil respiration into plant and soil components using natural abundance of ^{13}C. *Soil Science Society of American Journal* **63,** 1207–1213.

Ruimy A., Jarvis P.G. & Baldocchi D.D. (1995) CO_2 fluxes over plant canopies and solar radiation: a review. *Advances in Ecological Research* **26,** 1–68.

Schuepp P.H., Leclerc M.Y., MacPherson J.I. & Desjardins R.L. (1990) Footprint prediction of scalar fluxes from analytical solutions of the diffusion equation. *Boundary-Layer Meteorology* **50,** 355–373.

Shuttleworth W.J. & Wallace J.S. (1985) Evaporation from sparse crops – an energy combination theory. *Quarterly Journal of the Royal Meteorological Society* **111,** 839–855.

Steduto P. & Hsiao T. (1998) Maize canopies under two soil water regimes. I. Diurnal patterns of energy balance, carbon dioxide flux, and canopy conductance. *Agricultural and Forest Meteorology* **89,** 169–184.

Twine T.E., Kustas W.P., Norman J.M., Cook D.R., Houser P.R., Meyers T.P., Prueger J.H., Starks P.J. & Wesely M.L. (2000) Correcting eddy-covariance flux underestimates over a grassland. *Agricultural and Forest Meteorology* **103,** 279–300.

Verma S.B. (1989) Aerodynamic resistances to transfers of heat, mass and momentum. In *Estimation of Aerial Evapotranspiration* (eds T.A. Black, D.L. Spittlehouse, M.D. Novak & D.T. Price), pp. 13–20. IAHS Press, Wallingford, CT, USA.

Wang Y.-P. & Leuning R. (1998) A two-leaf model for canopy conductance, photosynthesis and partitioning of available energy I: model description and comparison with a multilayered model. *Agricultural and Forest Meteorology* **91,** 89–111.

Yakir D. & Wang X. (1996) Fluxes of CO_2 and water between terrestrial vegetation and the atmosphere estimated form isotope measurements. *Nature* **380,** 515–517.

Received 5 November 2004; received in revised form 25 May 2005; accepted for publication 5 August 2005

APPENDIX I

The canopy stomatal conductance for water vapour (g_{cw}) was inverted from the Penman–Monteith equation:

$$\frac{1}{g_{cw}} = \frac{\rho C_p \mathrm{VPD}}{\gamma \lambda E} + \frac{(\beta s/\gamma) - 1}{g_a} \quad \text{(A1)}$$

where ρ is the air density (kg m^{-3}), C_p is the specific heat of air under constant pressure (J kg^{-1} K^{-1}), β is the Bowen-ratio, λ is the latent heat of vaporization (J kg^{-1}), E is the plant transpiration (mol m^{-2} s^{-1}), γ is the psychrometric constant, s is the rate of change of saturation vapour pressure with temperature (Pa K^{-1}) and VPD is the vapour pressure deficit (kP$_a$). The aerodynamic conductance g_a was determined from

$$1/g_a = 1/g_b + 1/g_e \quad \text{(A2)}$$

where g_b is the average boundary layer conductance of the canopy leaves, calculated according to Owen & Thompson (1963) and Verma (1989) as

$$1/g_b = B^{-1}/u_* \quad \text{(A3)}$$

where B^{-1} is the dimensionless Stanton number g_e is the eddy diffusive conductance,

$$1/ge = u/(u_*)^2 \quad \text{(A4)}$$

where u is the average horizontal wind velocity (m s^{-1}). The canopy stomatal conductance for CO_2 (g_c) was determined from $g_{cw}/(D_v/D_c)$, where D_v and D_c are the diffusion coefficients for water vapour and CO_2 in air, respectively (Price & Black 1990).

When soil evaporation is considerably small, λE in Eqn A1 can be replaced with the latent heat flux measurement over the whole canopy. We used the Shuttleworth & Wallace (1985) two-layer model to estimate the contribution of soil evaporation. Results showed that the soil evaporation accounted for 3 to 10% during the period of full canopy closure (LAI ≥ 2), which as a result would cause a 1.2–12.2% overestimation in g_c.

APPENDIX II

Uncertainty in g_c estimation

The total uncertainty in the canopy conductance estimation (σ_{g_c}) was propagated from the fluctuations in the individual variables, which was estimated following Bevington (1969),

$$\sigma_{g_c}^2 = \sum\left[\sigma_i\left(\frac{\partial g_c}{\partial x_i}\right)\right]^2 \quad \text{(A5)}$$

where x_i, i = 1, 2, . . . 5, indicates the five key variables, VPD, λE, H, u and u_*. σ_i denotes the uncertainty of variable x_i. The uncertainties of individual variables are assumed to be uncorrelated, and the partial derivatives in the parentheses are evaluated at the mean values. The contribution of each variable to the total uncertainty (p_i) is given by,

Table 4. Contributions of individual variables to the total uncertainty in g_c estimation. The uncertainty of u is taken as the precision of wind speed measurement from the CSAT3 sonic anemometer. The uncertainty of water vapour pressure deficit (VPD) is estimated from the precision of water vapour density measurement from the LI-7500 (2.41e-06 kg m^{-3}) using the ideal gas law. Uncertainties of fluxes are estimated to be 20% (Morgenstern *et al*. 2004). The uncertainty of u_* is estimated as $\sigma_{F_M}\partial u_*/\partial F_m$, where $F_M = -\overline{w'u'} = u_*^2$ and $\sigma_{F_M} = 20\%F_M$.

Variable x_i	Contribution p_i (%)
VPD	53.7
λE	44.8
H	1.4
u	< 0.001
u_*	0.2

$$p_i = \frac{\left[\sigma_i\left(\frac{\partial g_c}{\partial x_i}\right)\right]^2}{\sum\left[\sigma_i\left(\frac{\partial g_c}{\partial x_i}\right)\right]^2} \times 100(\%). \quad \text{(A6)}$$

The total uncertainty of g_c was calculated half-hourly and p_i is shown in Table 4.

The total uncertainty in g_c was typically 30% during the experimental period. The uncertainties in VPD and λE contributed the most to the total error, about 54% and 45%, respectively.

Uncertainty in isotopic flux partitioning and night-time regression model

Similarly, the total uncertainty in the isotopic partitioning (σ_{F_A}) was calculated as,

$$\sigma_{F_A}^2 = \sum\left[\sigma_i\left(\frac{\partial F_A}{\partial x_i}\right)\right]^2 \quad \text{(A7)}$$

where x_i denotes the variable examined here: δ_a, δ_N, δ_R, g_c and C_a. Although F_N can be associated with relatively large error, here we assume it represents the 'true' value.